Extreme ultraviolet and x-ray transition wavelengths in Rb XXIV*

Indu Khatri[a)], Arun Goyal[a)†], Sunny Aggarwal[a)c)], A. K. Singh[b)], and Man Mohan[a)]

[a)] *Department of Physics and Astrophysics, University of Delhi, Delhi-110007, India*
[b)] *Department of Physics, D.D.U. College, University of Delhi, Delhi-110015, India*
[c)] *Department of Physics, Shyamlal College, University of Delhi, Delhi-110032, India*

(Received 16 February 2015; revised manuscript received 20 May 2015; published online 20 August 2015)

Energy levels, radiative rates, oscillator strengths and line strengths are reported for transitions among the lowest 97 levels of the ($1s^2 2s^2 2p^6$) $3s^2 3p^2$, $3s^2 3p3d$, $3s3p^3$, $3p^4$, $3s3p^2 3d$, and $3s^2 3d^2$ configurations of Rb XXIV. A multiconfiguration Dirac–Fock (MCDF) method is adopted for the calculations. Radiative rates, oscillator strengths, and line strengths are provided for all electric dipole (E1), magnetic dipole (M1), electric quadrupole (E2), and magnetic quadrupole (M2) transitions from the ground level to all 97 levels, although calculations are performed for a much larger number of levels. To achieve the accuracy of the data, comparisons are provided with similar data obtained from the Flexible Atomic Code (FAC) and also with the available theoretical and experimental results. Our energy levels are found to be accurate to better than 1.2%. Wavelengths calculated are found to lie in EUV (extreme ultraviolet) and x-ray regions. Additionally, lifetimes for all 97 levels are obtained for the first time.

Keywords: atomic data, energy levels, transition probability

PACS: 32.70.Cs **DOI:** 10.1088/1674-1056/24/10/103202

1. Introduction

The studies of stellar and solar coronae have been intensified as a result of superb coronal spectra recorded by extreme ultraviolet (EUV) explorer satellite, the Chandra x-ray Observatory and the Solar Heliospheric Observatory (SOHO).[1,2] As satellite-borne telescopes and instruments have expanded the range of detectable radiations into the x-ray region, astrophysical interest in the spectra of multiply charged ions has increased. The Ultraviolet (UV) through EUV and soft x-ray emission lines are useful for providing detailed knowledge about coronal atmosphere. Stellar coronal spectra are found to be rich in emission lines from high ionization states of highly ionized species[3] of cosmically abundant elements such as C, Mg, Si, Fe, and Ni which radiate in the x-ray region.[4]

There is considerable interest in the accurate atomic data for highly stripped ions as excitation energies and oscillator strengths in these ions are helpful in estimating the energy loss through impurity ions in fusion plasmas, diagnostic determination and modeling of high temperature astrophysical and laboratory plasma[5–7] and also in determining the stellar envelope opacities.[8] Precision spectroscopy also requires accurate theoretical values both for astrophysical and beam foil measurements. An accurate determination of radiative transition properties for highly ionized Si-like ions are important as a number of these have been observed in solar corona, in tokamak discharges and in laser produced plasma. Emission lines from singly and multiply charged Si-like ions have been observed in solar corona and laser produced plasmas.[9–12] Moreover, lines from intercombination transitions in Si-like ions are found to be useful in understanding density fluctuations and other elementary processes occurring in interstellar and laboratory plasma.[13,14] Though silicon-like ions have been studied theoretically and experimentally, semi empirical methods with limited predictive power and accuracy have been employed to evaluate energy levels. Most of the studies of the ions of the Si-isoelectronic sequence, available in the literature, are limited to transitions involving few low lying states of the $n = 3$ subshell.[15–48]

There are only limited data available for Si-like Rb based on semi empirical methods. Huang,[20] performed fully relativistic ab initio calculations of energy levels and transition probabilities for 27 low lying levels of Si-like ions in a range of $Z = 15$–106 by using a multiconfiguration Dirac–Fock (MCDF) method. A systematic study of atomic binding energies of ground state configurations for the lithium-to-dubnium isoelectronic series was performed by Rodrigues *et al.*[49] Thomas *et al.*[50] calculated the ionization potentials for all the elements up to $Z = 103$ based on a simple spherical shell solution for neutral atoms. Wavelengths and transition rates for magnetic-dipole transitions (M1) within $3s^2 3p^n$ ground configurations of ionized Cu-to-Mo were predicted by Sugar and Kaufman.[51] Khan[42] observed the Si-like spectra of Cu-to-Mo in tokamak-generated plasmas, and Cu-to-As in laser-produced plasmas. Though the spectrum of Rb was not observed, from the rest of the data the interpolated values of wavelengths were derived for Si-like Rb. Biémont *et*

*The authors, Indu Khatri and Arun Goyal, were supported by the U. G. C., India for their Junior Research Fellowship and Man Mohan by the U.G.C. for Basic Science Research Fellowship.

†Corresponding author. E-mail: arun.goyal.du@gmail.com

© 2015 Chinese Physical Society and IOP Publishing Ltd

al.[52] derived new ionization potentials for many light ions ($3 \leq Z \leq 50$) by systematically considering the differences in the calculated *ab-initio* value among these potentials. A semi-empirical jj-relativistic approach was used to check the consistency among the published experimental values of the p^2, p^3, and p^4 isoelectronic sequences including the Si sequence.[53] Charro *et al.*[27] calculated oscillator strengths of $3s^23p^2$–$3s^23p3d$ and $3s^23p^2$–$3s^23p^24s$ transitions in the Si sequence (K VI–Xe XLI) by using the relativistic quantum defect orbital (RQDO) method and the MCDF approach.

As the data for Rb XXIV are scarce, in this paper we present data on the radiative transition properties for Si-like Rb obtained by using a fully relativistic multiconfiguration Dirac–Fock approach which seems to be one of most reliable methods among the various standard methods suitable for predicting atomic data for transitions in highly charged or heavy atoms. In the present work, we calculate level compositions, energy levels, lifetimes for the lowest 97 levels of Rb XXIV, which belong to $3s^23p^2$, $3s^23p3d$, $3s3p^3$, $3p^4$, $3s3p^23d$, and $3s^23d^2$ configurations. Wavelengths, transition probabilities and oscillator strengths are calculated for E1, M1, E2, and M2 transitions. The atomic data we provide in this paper have not been reported before and may be useful in plasma diagnostics and various other fields. A comparison has been made wherever possible, and good agreement was achieved. To achieve the accuracy of our results, calculations have also been performed with the flexible atomic code (FAC). We have also provided a detailed comparison of our theoretical calculations with the data available from the NIST (National Institute of Standards and Technology)[54] database. An outline of the computational method is presented in Section 2 and results are discussed in Sections 3, 4, and 5.

2. Theoretical method

To calculate atomic data, we use the MCDF method originally developed by Grant *et al.*[55] and revised by Norrington[56] which has successfully been used earlier by ourselves and others.[57–63] The relativistic effects and QED effects must be considered in the highly ionized atoms as the velocity of electrons in these cases is fast and the nuclear potential energy is very strong. MCDF is a fully relativistic method based on the jj-coupling scheme. It also includes the relativistic corrections arising due to the Breit interaction and QED effects (Vacuum Polarization and Lamb Shift). In our calculations, the extended average level (EAL) option has been adopted, in which a weighted (proportional to $2j+1$) trace of the Hamiltonian matrix is minimized by producing a compromised set of orbitals. The results are evaluated with the Babushkin gauge, which in the relativistic limit corresponds to the length form of matrix elements.

In the MCDF method,[64] the relativistic atomic state function Ψ for a state $|PJM\rangle$ is obtained as linear combinations of symmetry adapted configuration state functions (CSFs).

$$|\psi_\alpha(PJM)\rangle = \sum_{i=1}^{n_c} C_i(\alpha)\,|\gamma_i(PJM)\rangle\,, \tag{1}$$

where n_c is the number of CSFs; γ_i denotes the appropriate labeling of the configuration state function such as orbital occupancy, coupling scheme, etc.; J and M are the angular quantum numbers; P denotes the parity. The CSFs are obtained from products of one-electron Dirac orbitals. Configuration mixing coefficients $C_i(\alpha)$ can be obtained through the diagonalization of Dirac Coulomb Hamiltonian

$$H_{\rm DC} = \sum_{i=1}^{N}\left(c\boldsymbol{\alpha}_i\cdot\boldsymbol{p}_i + (\beta_i - 1)\,c^2 + V_i^N\right) + \sum_{i>j}^{N}\frac{1}{r_{ij}}, \tag{2}$$

where V^N denotes the electron–nucleus Coulomb interaction, α and β are the 4×4 Dirac matrices, and c is the speed of light in atomic units. The configuration state functions Φ, which are eigen functions of J^2, J_Z, and P are built as linear combinations of Slater determinants. A Slater determinant, in the Dirac–Fock model, is a product of one-electron Dirac orbitals.

$$\phi_{nkm} = \frac{1}{r}\begin{pmatrix} P_{nk}(r) & \chi_{km}(\hat{r}) \\ \mathrm{i}Q_{nk}(r) & \chi_{-km}(\hat{r}) \end{pmatrix}, \tag{3}$$

where n is the principal quantum number, k and m are the relativistic angular quantum number and its z component respectively, $k = \pm(j+1/2)$ for $l = j \pm 1/2$ with l and j being the orbital and total angular momenta of the electron, $P_{nk}(r)$ and $Q_{nk}(r)$ denote the large and small component one-electron radial wavefunctions and are obtained as a self-consistent field solution of one-electron Dirac–Fock equation,[64] and $\chi_{km}(\hat{r})$ are the spinor spherical harmonics in the lsj coupling scheme and expressed as

$$\chi_{km}(\hat{r}) = \chi_{km}(\theta,\phi,\sigma) \times \sum_{\sigma=\pm 1/2}\left\langle lm-\sigma\frac{1}{2}\sigma\middle|l\frac{1}{2}jm\right\rangle \mathrm{Y}_l^{m-\sigma}(\theta,\phi)\phi^\sigma. \tag{4}$$

The energy of the N-electron system is given as

$$E_\alpha^{PJM} = \left\langle\Psi_\alpha(PJM)\middle|H^{\rm DC}\middle|\Psi_\alpha(PJM)\right\rangle, \tag{5}$$

where the Hamiltonian matrix $H^{\rm DC}$ is expressed as

$$H^{\rm DC} = \left\langle\gamma_i(PJM)\middle|H^{\rm DC}\middle|\gamma_j(PJM)\right\rangle. \tag{6}$$

For the energy to be stationary with respect to variations in mixing co-efficients $C_i(\alpha)$ subject to orthonormality condition $(C_i(\alpha))^+ C_j(\alpha) = \delta_{ij}$, the following equation holds

$$(H^{\rm DC} - E_\alpha^{\rm DC} I)C_i = 0, \tag{7}$$

where I is the $n_c \times n_c$ unit matrix. The predicted atomic energy level E_α thus can now be taken to be eigenvalues of $H^{\rm DC}$.

Since no detailed results are available, to assess the accuracy of our results and to make comparisons, analogous calculations are performed by using the Flexible Atomic Code (FAC) of Gu.[65] It is also a fully relativistic configuration interaction program and provides the results for energy levels and transition probability values comparable to MCDF. In this case, the single electron-orbital radial wavefunctions are determined by using a self-consistent field method based on the Dirac formulation. The atomic state wavefunctions and energy levels are obtained by diagonalizing the Dirac–Coulomb Hamiltonian. There are no major discrepancies reported in the energy level and radiative rates results determined by the two codes.

3. Energy levels

In Table 1, we list our fine structure levels relative to the ground level for Rb XXIV using MCDF wavefunctions. Relativistic multiconfiguration Dirac–Fock (MCDF) self-consistent field (SCF) calculations are employed in calculating the transition energies and transition rates. MCDF SCF is effective in treating nondynamic correlation. As E2 transition rates depend on the fifth power of transition energy, the accurate calculations of transition energies are essential. MCDF involves relativistic, Dirac–Coulomb and Breit correlation energies and Lamb shift corrections in transition energy calculations, therefore it can provide accurate transition energies and transition rates among multiplet states of atoms for a wide range of ionizations. To achieve high accuracy with this method, various important configurations are used in our calculations. As found by various authors,[66,67] for the ground state configuration $3s^23p^2$, the largest interaction is from the highly excited $3p^4$ configuration. Also, the excited $3s^23p4s$ configuration is found to interact strongly with $3s3p^3$ configuration states.[68] As reported by Biémont,[15,16] the perturbation between $3s3p^3$ and $3s^23p3d$ is quite important. Therefore, all these configurations have been included in our MCDF calculations. The calculations involving one electron excitations are excluded by us due to their negligible contributions to the calculating of energy levels and oscillator strengths.

Table 1. Dirac–Coulomb (DC), Breit and Quantum Electrodynamics (QED) contributions to the MCDF energy (in Rydberg) for the lowest 97 levels as a function of the orbital set. The sum total is compared with FAC and other available results. All energies are relative to the ground state.

S. No.	Configuration	J	MCDF2				MCDF1	NIST	FAC	Ref. [20]
			DC	Breit	QED	Total				
1	$3s^23p^2\ ^3P$	0	–	–	–	–	–	–	–	–
2	$3s^23p^2\ ^3P$	1	0.7363	–0.0177	0.0013	0.7197	0.7241	0.7291	0.7213	0.7234
3	$3s^23p^2\ ^3P$	2	1.0014	–0.0223	0.0014	0.9805	0.9887	0.9808	0.9810	0.9875
4	$3s^23p^2\ ^1D$	2	1.9569	–0.0379	0.0026	1.9216	1.9319	1.9217	1.9220	1.9283
5	$3s^23p^2\ ^1S$	0	2.6301	–0.0342	0.0023	2.5983	2.5828	2.5724	2.5916	2.5990
6	$3s3p^3\ ^5S^o$	2	4.5608	–0.0077	–0.0171	4.5361	4.6274		4.5454	4.5522
7	$3s3p^3\ ^3D^o$	1	5.5879	–0.0066	-0.1540	5.5659	5.7518		5.5666	5.5861
8	$3s3p^{33}D^o$	2	5.7011	–0.0141	–0.0150	5.6720	5.8440		5.6745	5.6929
9	$3s3p^3\ ^3D^o$	3	5.9908	–0.0253	–0.0146	5.9510	6.1279		5.9535	5.9722
10	$3s3p^{33}P^o$		6.5900	–0.0165	–0.0148	6.5587	6.7613		6.5571	6.5728
11	$3s3p^3\ ^1D^o$	2	6.6495	–0.0267	–0.0108	6.6120	6.8412		6.6082	9.4725
12	$3s3p^3\ ^3P^o$	1	6.6900	–0.0218	–0.0145	6.6537	6.8634		6.6519	6.6703
13	$3s3p^3\ ^3P^o$	2	7.2852	–0.0383	–0.0074	7.2396	7.4669		7.2345	6.6324
14	$3s^23p\ (^2_1P)\ 3d\ ^3F^o$	2	7.6481	–0.0395	–0.0033	7.6053	7.8589		7.5947	7.6325
15	$3s3p^3\ ^3S^o$	1	7.7114	–0.0123	–0.0166	7.6825	8.0537	7.5945	7.6649	8.5238
16	$3s^23p\ (^2_1P)\ 3d\ ^3F^o$	3	7.9016	–0.0486	–0.0005	7.8536	8.0992		7.8406	7.8850
17	$3s^23p\ (^2_1P)\ 3d\ ^3P^o$	2	8.4856	–0.0361	–0.0034	8.4461	8.7484	8.3757	8.4269	8.4691
18	$3s^23p\ (^2_1P)\ 3d\ ^3D^o$	1	8.5343	–0.0311	–0.0027	8.5004	8.7797		8.4768	9.3355
19	$3s^23p\ (^2_1P)\ 3d\ ^3F^o$	4	8.5631	–0.0665	–0.0017	8.4983	8.7947		8.4866	8.5290
20	$3s3p^3\ ^1P^o$	1	8.7434	–0.0333	–0.0115	8.6985	9.0602		8.6801	7.6934
21	$3s^23p\ (^2_1P)\ 3d\ ^1D^o$	2	9.1847	–0.0447	–0.0032	9.1367	9.5198	9.0584	9.1184	7.2616
22	$3s^23p\ (^2_1P)\ 3d\ ^3P^o$		9.2355	–0.0458	–0.0001	9.1896	9.5217		9.1715	9.2058
23	$3s^23p\ (^2_1P)\ 3d\ ^3D^o$	3	9.2970	–0.0557	–0.0003	9.2410	9.5773	9.1682	9.2201	9.2687
24	$3s^23p\ (^2_1P)\ 3d\ ^3P^o$	1	9.3625	–0.0499	–0.0016	9.3111	9.6462		9.2926	8.7200
25	$3s^23p\ (^2_1P)\ 3d\ ^3D^o$	2	9.5022	–0.0552	–0.0024	9.4445	9.8193	9.3740	9.4263	9.1629
26	$3s^23p\ (^2_1P)\ 3d\ ^1F^o$	3	10.0569	–0.0592	–0.0013	9.9990	10.3317	9.8952	9.9678	10.0196
27	$3s^23p\ (^2_1P)\ 3d\ ^1P^o$	1	10.3775	–0.0527	–0.0011	10.3237	10.7094		10.2821	10.3289
28	$3p^4\ ^3P$	2	10.9738	–0.0092	–0.0279	10.9366	11.0018		10.9293	
29	$3s3p^2\ (^3_2P)\ 3d\ ^5F$	1	11.1525	–0.0170	–0.0183	11.1172	11.1302		11.1008	
30	$3s3p^2\ (^3_2P)\ 3d\ ^5F$	2	11.3001	–0.0222	–0.0189	11.2589	11.2790		11.2438	
31	$3s3p^2\ (^3_2P)\ 3d\ ^5F$	3	11.5098	–0.0312	–0.0180	11.4605	11.4747		11.4451	
32	$3p^4\ ^3P$	0	11.6042	–0.0146	–0.0264	11.5632	11.6362		11.5547	

Table 1. (*Continued*).

S. No.	Configuration	J	MCDF2				MCDF1	NIST	FAC	Ref. [20]
			DC	Breit	QED	Total				
33	$3s3p^2\ (^3_2P)\ 3d\ ^3P$	1	11.6946	–0.0263	–0.0227	11.6456	11.6820		11.6357	
34	$3s3p^2\ (^3_2P)\ 3d\ ^5D$	2	11.8732	–0.0299	–0.0209	11.8224	11.8290		11.8038	
35	$3s3p^2\ (^3_2P)\ 3d\ ^5F$	4	11.8801	–0.0443	–0.0173	11.8185	11.8693		11.8100	
36	$3s3p^2\ (^3_2P)\ 3d\ ^5D$	0	11.9178	–0.0256	–0.0201	11.8721	11.9210		11.8606	
37	$3s3p^2\ (^3_2P)\ 3d\ ^5D$	3	11.9760	–0.0372	–0.0173	11.9215	11.9516		11.9042	
38	$3s3p^2\ (^3_2P)\ 3d\ ^5D$	1	12.0028	–0.0321	–0.0208	11.9499	11.9873		11.9392	
39	$3p^4\ ^1D$	2	12.0234	–0.0312	–0.0231	11.9692	12.0400		11.9595	
40	$3s3p^2\ (^3_2P)\ 3d\ ^5D$	4	12.1733	–0.0456	–0.0169	12.1108	12.1432		12.0936	
41	$3s3p^2\ (^3_2P)\ 3d\ ^5F$	5	12.2406	–0.0573	–0.0169	12.1664	12.1826		12.1498	
42	$3s3p^2\ (^3_2P)\ 3d\ ^3F$	2	12.2614	–0.0367	–0.0171	12.2077	12.2753		12.1840	
43	$3s3p^2\ (^1_2D)\ 3d\ ^3F$	3	12.5371	–0.0453	–0.0166	12.4752	12.5395		12.4520	
44	$3s3p^2\ (^3_2P)\ 3d\ ^5P$	3	12.7571	–0.0458	–0.0170	12.6943	12.7528		12.6737	
45	$3s3p^2\ (^3_2P)\ 3d\ ^5P$	2	12.8369	–0.0399	–0.0172	12.7799	12.8427		12.7575	
46	$3s3p^2\ (^3_2P)\ 3d\ ^5P$	1	12.9038	–0.0372	–0.0169	12.8497	12.9115		12.8268	
47	$3s3p^2\ (^3_2P)\ 3d\ ^3P$	2	12.9281	–0.0269	–0.0224	12.8789	13.0148		12.8585	
48	$3s3p^2\ (^1_2D)\ 3d\ ^3F$	4	13.0405	–0.0605	–0.0156	12.9644	13.0805		12.9420	
49	$3p^4\ ^1S$	0	13.2599	–0.0399	–0.0230	13.1970	13.3580		13.1818	
50	$3p^4\ ^3P$	1	13.3210	–0.0304	–0.0211	13.2695	13.4498		13.2448	
51	$3s3p^2\ (^3_2P)\ 3d\ ^3D$	2	13.4328	–0.0295	–0.0177	13.3856	13.5074		13.3431	
52	$3s3p^2\ (^1_2D)\ 3d\ ^3G$	3	13.4546	–0.0354	–0.0175	13.4017	13.5321		13.3614	
53	$3s3p^2\ (^1_2D)\ 3d\ ^3G$	4	13.6647	–0.0478	–0.0168	13.6001	13.7184		13.5622	
54	a	3	13.7263	–0.0429	–0.0173	13.6662	13.7680		13.6250	
55	$3s3p^2\ (^3_2P)\ 3d\ ^3D$	1	13.7889	–0.0425	–0.0169	13.7295	13.8220		13.6972	
56	$3s3p^2\ (^1_2D)\ 3d\ ^1G$	4	13.8172	–0.0533	–0.0150	13.7489	13.8412		13.7059	
57	$3s3p^2\ (^1_2D)\ 3d\ ^3P$	0	13.8619	–0.0409	–0.0201	13.8009	13.9795		13.7812	
58	$3s3p^2\ (^1_2D)\ 3d\ ^1F$	3	13.8977	–0.0450	–0.0166	13.8362	13.9834		13.7923	
59	$3s3p^2\ (^1_2D)\ 3d\ ^3G$	5	13.9461	–0.0597	–0.0166	13.8698	13.9804		13.8332	
60	$3s3p^2\ (^1_2D)\ 3d\ ^3D$	2	13.9684	–0.0446	–0.0162	13.9076	14.0443		13.8723	
61	$3s3p^2\ (^3_2P)\ 3d\ ^3D$	1	14.0697	–0.0284	–0.0178	14.0235	14.1756		13.9698	
62	$3s3p^2\ (^1_2D)\ 3d\ ^3D$	1	14.1251	–0.0367	–0.0176	14.0707	14.2610		14.0295	
63	$3s3p^2\ (^1_2D)\ 3d\ ^3D$	3	14.1626	–0.0485	–0.0163	14.0978	14.2579		14.0595	
64	$3s3p^2\ (^3_2P)\ 3d\ ^3P$	0	14.2045	–0.0386	–0.0169	14.1490	14.3120		14.1084	
65	b	2	14.2419	–0.0416	–0.0174	14.1829	14.3267		14.1404	
66	$3s3p^2\ (^1_2D)\ 3d\ ^3P$	1	14.3283	–0.0430	–0.0155	14.2697	14.4029		14.2250	
67	$3s3p^2\ (^1_2D)\ 3d\ ^3P$	2	14.4920	–0.0441	–0.0163	14.4316	14.5895		14.3841	
68	$3s3p^2\ (^3_2P)\ 3d\ ^3F$	2	14.5486	–0.0364	–0.0161	14.4962	14.6197		14.4511	
69	$3s3p^2\ (^3_2P)\ 3d\ ^3F$	4	14.5874	–0.0597	–0.0142	14.5134	14.6918		14.4703	
70	$3s3p^2\ (^3_2P)\ 3d\ ^3F$	3	14.5978	–0.0392	–0.0173	14.5413	14.7385		14.4949	
71	$3s3p^2\ (^1_2D)\ 3d\ ^3S$	1	14.6652	–0.0401	–0.0173	14.6078	14.7832		14.5586	
72	$3s3p^2\ (^3_2P)\ 3d\ ^3D$	2	14.7321	–0.0419	–0.0168	14.6734	14.8363		14.6220	
73	$3s3p^2\ (^3_2P)\ 3d\ ^3D$	3	14.7907	–0.0573	–0.0162	14.7171	14.8309		14.6720	
74	$3s3p^2\ (^1_2D)\ 3d\ ^1P$	1	14.9619	–0.0526	–0.0167	14.8926	15.0694		14.8441	
75	$3s3p^2\ (^1_2D)\ 3d\ ^1D$	2	15.1910	–0.0532	–0.0151	15.1227	15.3937		15.0831	
76	$3s3p^2\ (^3_2P)\ 3d\ ^3F$	4	15.2622	–0.0610	–0.0163	15.1849	15.4250		15.1381	
77	$3s3p^2\ (^1S)\ 3d\ ^3D$	3	15.3231	–0.0570	–0.0162	15.2500	15.4463		15.1990	
78	$3s3p^2\ (^1_2D)\ 3d\ ^1S$	0	15.4925	–0.0317	–0.0201	15.4408	15.7439		15.4054	
79	$3s3p^2\ (^3_2P)\ 3d\ ^3D$	3	15.5872	–0.0553	–0.0155	15.5164	15.7775		15.4623	
80	$3s3p^2\ (^1S)\ 3d\ ^3D$	2	15.6482	–0.0495	–0.0152	15.5834	15.8114		15.5327	
81	$3s3p^2\ (^3_2P)\ 3d\ ^1P$	1	15.6882	–0.0391	–0.0174	15.6317	15.8091		15.5680	
82	$3s3p^2\ (^1S)\ 3d\ ^1D$	2	15.7028	–0.0493	–0.0169	15.6366	15.8795		15.5796	
83	$3s3p^2\ (^1S)\ 3d\ ^3D$	1	15.8089	–0.0452	–0.0169	15.7468	15.9718		15.6938	
84	$3s3p^2\ (^3_2P)\ 3d\ ^3P$	2	16.0174	–0.0484	–0.0177	15.9513	16.3002		15.8900	
85	$3s3p^2\ (^3_2P)\ 3d\ ^3P$	1	16.3817	–0.0516	–0.0175	16.3126	16.6298		16.2432	
86	$3s3p^2\ (^3_2P)\ 3d\ ^3P$	0	16.4470	–0.0468	–0.0190	16.3811	16.7168		16.3298	
87	$3s3p^2\ (^3_2P)\ 3d\ ^1F$	3	16.5089	–0.0538	–0.0156	16.4395	16.7573		16.3771	
88	$3s^23d^2\ ^3F$	2	16.5381	–0.0614	–0.0052	16.4714	16.7709		16.3934	
89	$3s^23d^2\ ^3F$	3	16.6774	–0.0699	–0.0052	16.6023	16.8579		16.5246	
90	$3s^23d^2\ ^3F$	4	16.7488	–0.0822	–0.0023	16.6637	16.8967		16.5827	
91	$3s3p^2\ (^3_2P)\ 3d\ ^1D$	2	17.0270	–0.0554	–0.0123	16.9593	17.3016		16.8708	
92	$3s^23d^2\ ^3P$	0	17.0840	–0.0623	–0.0036	17.0181	17.3274		16.9280	
93	$3s^23d^2\ ^3P$	1	17.1468	–0.0656	–0.0034	17.0778	17.3657		16.9853	
94	$3s^23d^2\ ^1G$	4	17.2124	–0.0793	–0.0024	17.1307	17.3858		17.0513	
95	$3s^23d^2\ ^3P$	2	17.2434	–0.0642	–0.0087	17.1705	17.5574		17.0864	
96	$3s^23d^2\ ^1D$	2	17.3800	–0.0733	–0.0055	17.3012	17.6530		17.2150	
97	$3s^23d^2\ ^1S$	0	17.4768	–0.0183	–0.0334	17.4251	18.7066		17.3985	

a: unidentified level at position 54, b: unidentified level at position 65.

For reliable calculations and to form a reasonable correlation model, calculations are performed by taking two different sets of configurations. In the first set of calculations, we use 6 configurations ($1s^22s^22p^6$) $3s^23p^2$, $3s^23p3d$, $3s3p^3$, $3p^4$, $3s3p^23d$, and $3s^23d^2$ referred to as MCDF1, which are listed in Table 1. For convergence, we perform another set of similar calculations, including some additional configurations namely $3s3p3d^2$, $3s3d^3$, $3p3d^3$, $3p^23d^2$, $3p^33d$, $3d^4$, $3s^23p4s$, $3s^23p4p$, $3s^23p4d$, $3s^23p4f$, $3s3p^24s$, $3s3p^24p$, $3s3p^24d$, and $3s3p^24f$ referred to as MCDF2. As the results are found to be better for MCDF2 with stronger configuration interaction (CI) included in the calculations, we use MCDF2 for all our calculations. In MCDF2, we include CI among 20 configurations, keeping [$1s^22s^22p^6$] frozen, namely $3s^23p^2$, $3s3p^3$, $3p^4$, $3s^23p3d$, $3s^23d^2$, $3s3p^23d$, $3s3p3d^2$, $3s3d^3$, $3p3d^3$, $3p^23d^2$, $3p^33d$, $3d^4$, $3s^23p4s$, $3s^23p4p$, $3s^23p4d$, $3s^23p4f$, $3s3p^24s$, $3s3p^24p$, $3s3p^24d$, and $3s3p^24f$ which generate 730 energy levels. Among these levels, we consider the lowest 97 fine-structure levels belonging to $3s^23p^2$, $3s^23p3d$, $3s3p^3$, $3p^4$, $3s3p^23d$, and $3s^23d^2$configurations for our calculations. We perform similar calculations by using FAC which includes 3*4, $3s^23p$ 4*1, $3s3p^2$ 4*1, $3s3d^2$ 4*1, $3s^23d$ 4*1, $3p^3$ 4*1, and $3d^3$ 4*1, which generate 4363 levels.

In Table 1, we list our calculated excitation energies of the fine structure levels obtained from the MCDF method with and without including Breit and QED effects for MCDF2. Before we discuss our results further, we note that Huang[20] calculated the energy levels for 27 low lying levels of Rb XXIV. However, these results are unreliable as can be seen from Table 1. Therefore, we do not discuss these results further. We find that our Breit and QED corrected energies are lower than the corresponding coulomb energies by up to ~ 0.08 Ryd. Our level energies without the Breit and QED effects are higher than the NIST values by ~ 0.16 Ryd. The energies are lowered by a maximum value of 0.08 Ryd with including the Breit and QED effects, which shows the importance of including higher relativistic effects for heavy ions. Further, it is seen that QED corrections are comparable to or greater than those with including the Breit effect for levels where single and double electron excitations from 3s to 3p and 3d orbitals occur, such as for levels $3s3p^3\ ^3D^o_2$, $3s3p^3\ ^3P^o_0$, and $3s3p^2\ (^3_2P)\ 3d\ ^3P_1$ whereas QED corrections are smaller for levels formed due to excitations from 3p to a higher orbital such as $3s^23d^2\ ^3F_{2,3}$. Energies obtained with including the Breit and QED effects are lower than the NIST values by 1.2%. Unfortunately, data available on NIST are limited to only a few levels. One can see that the energy values obtained from the FAC code agree well with our MCDF2 results within 0.54%. The level ordering is found to be generally the same except at a few places between the two calculations. Differences between the calculations occur due to the different ways in which the central potentials for radial orbitals and recoupling schemes of angular parts are calculated. Considering the results of NIST as a standard reference for comparison we find that the agreement of our MCDF2 energy levels with NIST results is within 1.2% which shows the reliability of our levels.

We also list the mixing coefficients for these 97 levels in Table 2. Under the column LSJ coupling the first number of each entry denotes the leading percentage of the level corresponding to the level number in the first column. The next leading percentage is in the form P(Q) where the next leading percentage is P% of Q level number in the first column. We note that some of the levels are easily identifiable such as $3s^23p\ (^2_1P)\ 3d\ ^3F^o_2$ due to clear dominance. For many levels, the mixing of eigenvectors from different levels is very strong. For example, $3s3p^3\ ^1D^o_2$ is strongly coupled with $3s3p^3\ ^1P^o_2$ and $3s^23p\ (^2_1P)\ 3d\ ^1D^o_2$ with their mixing being 27%, 22%, and 20% respectively. Further, we notice that due to the strong mixing among the levels $3s^23p\ (^2_1P)\ 3d\ ^5D_2$, and $3p^4\ ^1D_2$, these levels can be interchanged. Sometimes the same eigenvector dominates over several levels and the identification of such levels is ambiguous as levels Nos. 54 and 65 are unidentifiable in our calculations. There remains scope for re-designation as the identification is not unique for a few levels. The corresponding *jj* designations for the levels have also been provided under the column "*JJ* coupling" as the *LSJ* coupling is not found to be accurate for highly mixed levels. Under this column, the first number represents the leading percentage of the level and p^-, p, d^-, d denote $p_{1/2}$, $p_{3/2}$, $d_{3/2}$, and $d_{5/2}$ respectively.

Table 2. Level Nos., Wave-function compositions and lifetimes of the first 97 fine structure levels of Rb XXIV using MCDF2.

S. No.	Configurations	*J*	Lifetime	Composition	
				JJ coupling	*LSJ* coupling
1	$3s^23p^2\ ^3P$	0	–	93 $3s^23p^{-2}$	83
2	$3s^23p^2\ \ ^3P$	1	1.33×10^{-4}	98 $3s^23p^{-1}3p^1$	98
3	$3s^23p^2\ ^3P$	2	5.21×10^{-3}	92 $3s^23p^{-1}3p^1$	56+41(4)
4	$3s^23p^2\ ^1D$	2	4.23×10^{-5}	91 $3s^23p^2$	56+41(3)
5	$3s^23p^2\ ^1S$	0	1.41×10^{-5}	92 $3s^23p^2$	82
6	$3s3p^3\ ^5S^o$	2	1.69×10^{-9}	56 $3s^13p^{-2}3p^1$	85
7	$3s3p^3\ ^3D^o$	1	1.07×10^{-10}	58 $3s^13p^{-2}3p^1$	66
8	$3s3p^3\ ^3D^o$	2	2.10×10^{-10}	57 $3s^13p^{-1}3p^2$	64
9	$3s3p^3\ ^3D^o$	3	2.72×10^{-10}	88 $3s^13p^{-1}3p^2$	88
10	$3s3p^3\ ^3P^o$	0	7.19×10^{-11}	89 $3s^13p^{-1}3p^2$	89

Table 2. (*Continued*).

S. No.	Configurations	J	Lifetime	Composition	
				JJ coupling	*LSJ* coupling
11	$3s3p^3\ ^1D^o$	2	9.38×10^{-11}	27 $3s^1 3p^{-1} 3p^2$	27+22(13)+20(21)
12	$3s3p^3\ ^3P^o$	1	5.76×10^{-11}	52 $3s^1 3p^{-1} 3p^2$	69
13	$3s3p^3\ ^3P^o$	2	1.66×10^{-10}	46 $3s^1 3p^3$	33+23(14)+21(21)
14	$3s^2 3p\ (^2_1P)\ 3d\ ^3F^o$	2	8.08×10^{-11}	40 $3s^2 3p^{-1} 3d^{-1}$	66+17(11)
15	$3s3p^3\ ^3S^o$	1	7.26×10^{-12}	41 $3s^1 3p^{-1} 3p^2$	56+32(20)
16	$3s^2 3p\ (^2_1P)\ 3d\ ^3F^o$	3	1.44×10^{-10}	67 $3s^2 3p^{-1} 3d^1$	91
17	$3s^2 3p\ (^2_1P)\ 3d\ ^3P^o$	2	9.29×10^{-12}	73 $3s^2 3p^{-1} 3d^1$	49+19(25)
18	$3s^2 3p\ (^2_1P)\ 3d\ ^3D^o$	1	7.60×10^{-12}	75 $3s^2 3p^{-1} 3d^1$	35+28(24)+16(27)
19	$3s^2 3p\ (^2_1P)\ 3d\ ^3F^o$	4	1.22×10^{-4}	98 $3s^2 3p^1 3d^1$	98
20	$3s3p^3\ ^1P^o$	1	7.13×10^{-12}	44 $3s^1 3p^3$	41+30(15)+23(18)
21	$3s^2 3p\ (^2_1P)\ 3d\ ^1D^o$	2	6.27×10^{-12}	61 $3s^2 3p^1 3d^{-1}$	28+39(25)+20(11)
22	$3s^2 3p\ (^2_1P)\ 3d\ ^3P^o$	0	8.85×10^{-12}	88 $3s^2 3p^1 3d^{-1}$	88
23	$3s^2 3p\ (^2_1P)\ 3d\ ^3D^o$	3	7.35×10^{-12}	38 $3s^2 3p^1 3d^{-1}$	74
24	$3s^2 3p\ (^2_1P)\ 3d\ ^3P^o$	1	8.12×10^{-12}	66 $3s^2 3p^1 3d^{-1}$	58+20(18)
25	$3s^2 3p\ (^2_1P)\ 3d\ ^3D^o$	2	8.42×10^{-12}	61 $3s^2 3p^1 3d^1$	25+37(17)
26	$3s^2 3p\ (^2_1P)\ 3d\ ^1F^o$	3	7.33×10^{-12}	53 $3s^2 3p^1 3d^1$	86
27	$3s^2 3p\ (^2_1P)\ 3d\ ^1P^o$	1	8.21×10^{-12}	69 $3s^2 3p^1 3d^1$	76
28	$3p^4\ ^3P$	2	5.69×10^{-11}	54 $3p^{-2} 3p^2$	42+28(47)
29	$3s3p^2\ (^3_2P)\ 3d\ ^5F$	1	6.85×10^{-10}	63 $3s^1 3p^{-2} 3d^{-1}$	84
30	$3s3p^2\ (^3_2P)\ 3d\ ^5F$	2	2.18×10^{-10}	29 $3s^1 3p^{-2} 3d^{-1}$	75
31	$3s3p^2\ (^3_2P)\ 3d\ ^5F$	3	3.10×10^{-10}	41 $3s^1 3p^{-2} 3d^1$	69+22(37)
32	$3p^4\ ^3P$	0	4.79×10^{-11}	42 $3p^{-2} 3p^2$	36+26(64)
33	$3s3p^2\ (^3_2P)\ 3d\ ^3P$	1	9.28×10^{-11}	32 $3s^1 3p^{-1} 3p^1\ (3/2)\ 3d^{-1}$	34+31(50)+22(38)
34	$3s3p^2\ (^3_2P)\ 3d\ ^5D$	2	1.28×10^{-10}	21 $3s^1 3p^{-1} 3p^1\ (3/2)\ 3d^{-1}$	33+20(39)
35	$3s3p^2\ (^3_2P)\ 3d\ ^5F$	4	5.74×10^{-9}	51 $3s^1 3p^{-1} 3p^1\ (3/2)\ 3d^1$	82
36	$3s3p^2\ (^3_2P)\ 3d\ ^5D$	0	8.45×10^{-11}	34 $3s^1 3p^{-1} 3p^1\ (3/2)\ 3d^{-1}$	80
37	$3s3p^2\ (^3_2P)\ 3d\ ^5D$	3	1.15×10^{-10}	41 $3s^1 3p^{-1} 3p^1\ (5/2)\ 3d^{-1}$	42+23(31)
38	$3s3p^2\ (^3_2P)\ 3d\ ^5D$	1	6.72×10^{-11}	21 $3s^1 3p^{-1} 3p^1\ (5/2)\ 3d^1$	64+21(50)
39	$3p^4\ ^1D$	2	6.72×10^{-11}	35 $3p^{-1} 3p^3$	27+28(34)
40	$3s3p^2\ (^3_2P)\ 3d\ ^5D$	4	1.52×10^{-9}	36 $3s^1 3p^{-1} 3p^1\ (5/2)\ 3d^1$	55+22(48)
41	$3s3p^2\ (^3_2P)\ 3d\ ^5F$	5	2.16×10^{-9}	62 $3s^1 3p^{-1} 3p^1\ (5/2)\ 3d^1$	91
42	$3s3p^2\ (^3_2P)\ 3d\ ^3F$	2	1.38×10^{-10}	28 $3s^1 3p^{-1} 3p^1\ (3/2)\ 3d^1$	38+37 (a)
43	$3s3p^2\ (^1_2D)\ 3d\ ^3F$	3	3.54×10^{-11}	45 $3s^1 3p^{-1} 3p^1\ (3/2)\ 3d^1$	32+26 (b)+24(44)
44	$3s3p^2\ (^3_2P)\ 3d\ ^5P$	3	1.27×10^{-11}	36 $3s^1 3p^{-1} 3p^1\ (5/2)\ 3d^1$	55+25(37)
45	$3s3p^2\ (^3_2P)\ 3d\ ^5P$	2	9.23×10^{-12}	34 $3s^1 3p^{-1} 3p^1\ (5/2)\ 3d^{-1}$	80
46	$3s3p^2\ (^3_2P)\ 3d\ ^5P$	1	8.26×10^{-12}	54 $3s^1 3p^{-1} 3p^1\ (5/2)\ 3d^{-1}$	88
47	$3s3p^2\ (^3_2P)\ 3d\ ^3P$	2	9.17×10^{-12}	23 $3s^1 3p^{-1} 3p^1\ (5/2)\ 3d^1$	24+26(28)
48	$3s3p^2\ (^1_2D)\ 3d\ ^3F$	4	6.99×10^{-10}	69 $3s^1 3p^2\ 3d^1$	26+27(69)+28(40)
49	$3p^4\ ^1S$	0	3.88×10^{-11}	56 $3s^1 3p^2\ 3d^1$	38+35(64)
50	$3p^4\ ^3P$	1	8.74×10^{-12}	21 $3p^{-1} 3p^3$	21
51	$3s3p^2\ (^3_2P)\ 3d\ ^3D$	2	1.45×10^{-11}	23 $3s^1 3p^{-2} 3d^1$	22+21(68)
52	$3s3p^2\ (^1_2D)\ 3d\ ^3G$	3	2.83×10^{-11}	43 $3s^1 3p^{-1} 3p^1\ (3/2)\ 3d^{-1}$	75
53	$3s3p^2\ (^1_2D)\ 3d\ ^3G$	4	3.66×10^{-11}	26 $3s^1 3p^{-1} 3p^1\ (5/2)\ 3d^{-1}$	82
54	b	3	1.36×10^{-11}	31 $3s^1 3p^{-1} 3p^1\ (3/2)\ 3d^{-1}$	
55	$3s3p^2\ (^3_2P)\ 3d\ ^3D$	1	1.45×10^{-11}	25 $3s^1 3p^2\ 3d^{-1}$	33+20(66)+17(83)
56	$3s3p^2\ (^1_2D)\ 3d\ ^1G$	4	5.38×10^{-11}	25 $3s^1 3p^{-1} 3p^1\ (3/2)\ 3d^1$	61
57	$3s3p^2\ (^1_2D)\ 3d\ ^3P$	0	1.06×10^{-11}	33 $3s^2 3d^2$	33+26(32)
58	$3s3p^2\ (^1_2D)\ 3d\ ^1F$	3	1.34×10^{-11}	47 $3s^1 3p^{-1} 3p^1\ (3/2)\ 3d^1$	32
59	$3s3p^2\ (^1_2D)\ 3d\ ^3G$	5	5.62×10^{-11}	62 $3s^1 3p^2\ 3d^1$	91
60	$3s3p^2\ (^1_2D)\ 3d\ ^3D$	2	9.10×10^{-12}	44 $3s^1 3p^2\ 3d^{-1}$	34
61	$3s3p^2\ (^3_2P)\ 3d\ ^3D$	1	8.58×10^{-12}	29 $3s^1 3p^{-1} 3p^1\ (1/2)\ 3d^{-1}$	28+32(62)
62	$3s3p^2\ (^1_2D)\ 3d\ ^3D$	1	9.62×10^{-12}	30 $3s^1 3p^{-1} 3p^1\ (3/2)\ 3d^1$	47+25(55)
63	$3s3p^2\ (^1_2D)\ 3d\ ^3D$	3	8.47×10^{-12}	34 $3s^1 3p^2\ 3d^{-1}$	45+18 (b)
64	$3s3p^2\ (^3_2P)\ 3d\ ^3P$	0	9.27×10^{-12}	49 $3s^1 3p^{-1} 3p^1\ (5/2)\ 3d^1$	23+37(57)
65	c	2	1.10×10^{-11}	35 $3s^1 3p^{-1} 3p^1\ (3/2)\ 3d^1$	
66	$3s3p^2\ (^1_2D)\ 3d\ ^3P$	1	1.04×10^{-11}	29 $3s^1 3p^{-1} 3p^1\ (3/2)\ 3d^1$	36+17(33)
67	$3s3p^2\ (^1_2D)\ 3d\ ^3P$	2	9.72×10^{-12}	14 $3s^1 3p^2\ 3d^{-1}$	21+20(72)
68	$3s3p^2\ (^3_2P)\ 3d\ ^3F$	2	6.90×10^{-12}	45 $3s^1 3p^{-1} 3p^1\ (1/2)\ 3d^{-1}$	34
69	$3s3p^2\ (^3_2P)\ 3d\ ^3F$	4	8.64×10^{-12}	56 $3s^1 3p^2\ 3d^{-1}$	58
70	$3s3p^2\ (^3_2P)\ 3d\ ^3F$	3	7.93×10^{-12}	28 $3s^1 3p^{-1} 3p^1\ (1/2)\ 3d^1$	39+25(77)
71	$3s3p^2\ (^1_2D)\ 3d\ ^3S$	1	8.04×10^{-12}	19 $3s^1 3p^{-1} 3p^1\ (3/2)\ 3d^{-1}$	28+17(61)
72	$3s3p^2\ (^3_2P)\ 3d\ ^3D$	2	8.70×10^{-12}	26 $3s^1 3p^{-1} 3p^1\ (1/2)\ 3d^1$	24+18(80)

Table 2. (*Continued*).

S. No.	Configurations	J	Lifetime	Composition	
				JJ coupling	*LSJ* coupling
73	$3s3p^2$ ($^3_2$P) 3d ^{3}D	3	1.56×10^{-11}	56 $3s^13p^2$ $3d^1$	39
74	$3s3p^2$ ($^1_2$D) 3d ^{1}P	1	9.32×10^{-12}	39 $3s^13p^2$ $3d^1$	17+48(71)
75	$3s3p^2$ ($^1_2$D) 3d ^{1}D	2	7.91×10^{-12}	25 $3s^13p^2$ $3d^1$	29+25(96)
76	$3s3p^2$ ($^3_2$P) 3d ^{3}F	4	8.66×10^{-12}	69 $3s^13p^2$ $3d^1$	86
77	$3s3p^2$ (^{1}S) 3d ^{3}D	3	9.65×10^{-12}	62 $3s^13p^2$ $3d^1$	49+20(79)
78	$3s3p^2$ ($^1_2$D) 3d ^{1}S	0	4.84×10^{-12}	22 $3s^13p^{-1}3p^1$ (3/2) $3d^{-1}$	32+31(86)+22(49)
79	$3s3p^2$ ($^3_2$P) 3d ^{3}D	3	6.39×10^{-12}	39 $3s^13p^2$ $3d^1$	55
80	$3s3p^2$ (^{1}S) 3d ^{3}D	2	6.22×10^{-12}	38 $3s^13p^2$ $3d^{-1}$	26+22(72)+21(51)
81	$3s3p^2$ ($^3_2$P) 3d ^{1}P	1	5.15×10^{-12}	41 $3s^13p^2$ $3d^{-1}$	24+23(83)+22(74)
82	$3s3p^2$ (^{1}S) 3d ^{1}D	2	6.90×10^{-12}	26 $3s^13p^{-1}3p^1$ (3/2) $3d^{-1}$	41+22(84)+19(72)
83	$3s3p^2$ (^{1}S) 3d ^{3}D	1	5.36×10^{-12}	34 $3s^13p^2$ $3d^{-1}$	19+35(61)
84	$3s3p^2$ ($^3_2$P) 3d ^{3}P	2	4.87×10^{-12}	37 $3s^13p^2$ $3d^1$	40
85	$3s3p^2$ ($^3_2$P) 3d ^{3}P	1	4.19×10^{-12}	39 $3s^13p^2$ $3d^1$	44+22(74)
86	$3s3p^2$ ($^3_2$P) 3d ^{3}P	0	3.75×10^{-12}	40 $3s^13p^2$ $3d^{-1}$	44
87	$3s3p^2$ ($^3_2$P) 3d ^{1}F	3	4.16×10^{-12}	37 $3s^13p^2$ $3d^{-1}$	64+17(58)
88	$3s^23d^2$ ^{3}F	2	4.51×10^{-12}	44 $3s^23d^{-2}$	66+17 (a)
89	$3s^23d^2$ ^{3}F	3	5.03×10^{-12}	65 $3s^23d^{-1}3d^1$	65+19(43)
90	$3s^23d^2$ ^{3}F	4	5.56×10^{-12}	55 $3s^23d^2$	77+17(48)
91	$3s3p^2$ ($^3_2$P) 3d ^{1}D	2	3.86×10^{-12}	17 $3s^13p^2$ $3d^1$	49
92	$3s^23d^2$ ^{3}P	0	3.87×10^{-12}	50 $3s^23d^{-2}$	74+19(57)
93	$3s^23d^2$ ^{3}P	1	4.04×10^{-12}	753$s^23d^{-1}3d^1$	75+20(66)
94	$3s^23d^2$ ^{1}G	4	7.49×10^{-12}	56 $3s^23d^{-1}3d^1$	80+16(56)
95	$3s^23d^2$ ^{3}P	2	4.01×10^{-12}	41 $3s^23d^{-1}3d^1$	36+17(91)
96	$3s^23d^2$ ^{1}D	2	4.39×10^{-12}	64 $3s^23d^2$	44+22(95)+19(75)
97	$3s^23d^2$ ^{1}S	0	3.50×10^{-11}	63 $3s^23d^2$	76+17(78)

The letters "a", "b", and "c" in the row *LSJ* coupling imply that a: $3s3p^2$ ($^1_2$D) 3d $^3F_2$, b: unidentified level at position 54, c: unidentified level at position 65.

4. Radiative rates

For a transition $i \rightarrow j$, the absorption oscillator strength f_{ij} (dimensionless), and radiative rate A_{ji} (in s^{-1}) are related by

$$f_{ij} = \frac{mc}{8\pi^2 e^2}\lambda_{ji}^2 \frac{w_j}{w_i} A_{ji} = 1.49\times10^{-16}\lambda_{ji}^2 (w_j/w_i) A_{ji}, \quad (8)$$

where m and e denote the electron mass and charge respectively, c is the velocity of light, λ_{ji} represents the transition wavelength in Å, and w_i and w_j are the statistical weights of the lower i and upper j levels respectively. The line strength S_{ij} and the oscillator strength f_{ij} obey the following relations:

(i) for electric dipole transitions (E1)

$$A_{ji} = \frac{2.0261\times10^{18}}{w_j\lambda_{ji}^3} S_{ij} \quad \text{and} \quad f_{ij} = \frac{303.75}{\lambda_{ji} w_i} S_{ij}; \quad (9)$$

(ii) for the magnetic dipole transitions (M1)

$$A_{ji} = \frac{2.6974\times10^{13}}{w_j\lambda_{ji}^3} S_{ij} \quad \text{and} \quad f_{ij} = \frac{4.044\times10^{-3}}{\lambda_{ji} w_i} S_{ij}; \quad (10)$$

(iii) for electric quadrupole transitions (E2)

$$A_{ji} = \frac{1.1199\times10^{18}}{w_j\lambda_{ji}^5} S_{ij} \quad \text{and} \quad f_{ij} = \frac{167.89}{\lambda_{ji}^3 w_i} S_{ij}; \quad (11)$$

(iv) for the magnetic quadrupole transitions (M2)

$$A_{ji} = \frac{1.4910\times10^{13}}{w_j\lambda_{ji}^5} S_{ij} \quad \text{and} \quad f_{ij} = \frac{2.236\times10^{-3}}{\lambda_{ji}^3 w_i} S_{ij}. \quad (12)$$

The wavelengths (λ in Å), radiative rates (A_{ji} in s^{-1}), oscillator strengths (f_{ij} dimensionless), line strengths (S_{ij} in atomic unit "a.u.") determined from the ground level for transitions among all the 97 levels considered in this paper by using MCDF wavefunctions are given in Tables 3 and 4. Some of the strong lines belonging to $n = 3 \rightarrow 3$ transition arrays of the silicon sequence which appears in laboratory plasma and in astrophysical sources are important for solar identifications. An intercombination, or spin-forbidden, line signals the breakdown of the spin conservation rule for transitions, due to the spin–orbit effect like spin-dependent interactions. In astrophysical precision spectroscopy and diagnostics of laboratory plasma, many lines are observed due to spin-forbidden transitions. These are useful in understanding density fluctuations and other elementary processes occurring in interstellar and laboratory plasmas. In the present work, we list the transition probabilities, oscillator strengths of such transitions like $3s^23p^2$ $^3P_0$-$3s3p^3$ $^5S^o_2$, $3s^23p^2$ $^3P_0$–$3s^23p3d$ $^5F_2$, $^5P_2$, $^5D_2$. As spin-forbidden transitions arise due to small mixing of states, such data can also be used for testing atomic theory.

Table 3. Transition data for E1 and E2 transitions for Si-like Rb from $3s^23p^2\ ^3P_o$: levels and J for lower level i, upper level k, wavelength λ (in Å), transition rate A_{ji} (length form), oscillator strength f_{ij} (length form), line strength S_{ij} (in atomic unit a.u.) (length form),

Levels		J		MCDF2				Vel/len	Transition type
i	k	i	k	λ/Å	A_{ji}/s^{-1}	f_{ij}	S_{ij}/a.u.		
$3s^23p^2\ ^3P$	$3s3p^3\ ^3D^o$	0	1	1.637×10^{2}	8.34×10^{9}	1.01×10^{-1}	5.42×10^{-2}	1.00	E1
$3s^23p^2\ ^3P$	$3s3p^3\ ^3P^o$	0	1	1.370×10^{2}	4.02×10^{9}	3.39×10^{-2}	1.53×10^{-2}	0.96	E1
$3s^23p^2\ ^3P$	$3s3p^3\ ^3S^o$	0	1	1.186×10^{2}	2.29×10^{10}	1.45×10^{-1}	5.66×10^{-2}	1.00	E1
$3s^23p^2\ ^3P$	$3s^23p\ (^2_1P)\ 3d\ ^3D^o$	0	1	1.072×10^{2}	1.18×10^{11}	6.08×10^{-1}	2.15×10^{-1}	1.00	E1
$3s^23p^2\ ^3P$	$3s3p^3\ ^1P^o$	0	1	1.047×10^{2}	9.32×10^{9}	4.60×10^{-2}	1.59×10^{-2}	1.10	E1
$3s^23p^2\ ^3P$	$3s^23p\ (^2_1P)\ 3d\ ^3P^o$	0	1	9.787×10^{1}	3.12×10^{8}	1.34×10^{-3}	4.33×10^{-4}	1.60	E1
$3s^23p^2\ ^3P$	$3s^23p\ (^2_1P)\ 3d\ ^1P^o$	0	1	8.827×10^{1}	1.67×10^{9}	5.86×10^{-3}	1.70×10^{-3}	0.97	E1
$3s^23p^2\ ^3P$	$3s^23p^2\ ^3P$	0	2	9.294×10^{2}	7.80×10^{0}	5.05×10^{-9}	2.41×10^{-2}	1.10	E2
$3s^23p^2\ ^3P$	$3s^23p^2\ ^1D$	0	2	4.742×10^{2}	2.42×10^{-5}	4.09×10^{-15}	2.60×10^{-9}	6400	E2
$3s^23p^2\ ^3P$	$3p^4\ ^3P$	0	2	8.332×10^{1}	6.20×10^{5}	3.23×10^{-6}	1.11×10^{-2}	0.91	E2
$3s^23p^2\ ^3P$	$3s3p^2\ (^3_2P)\ 3d\ ^5F$	0	2	8.094×10^{1}	1.25×10^{3}	6.11×10^{-9}	1.93×10^{-5}	1.20	E2
$3s^23p^2\ ^3P$	$3s3p^2\ (^3_2P)\ 3d\ ^5D$	0	2	7.708×10^{1}	1.81×10^{4}	8.07×10^{-8}	2.20×10^{-4}	1.20	E2
$3s^23p^2\ ^3P$	$3p^4\ ^1D$	0	2	7.613×10^{1}	1.20×10^{5}	5.22×10^{-7}	1.37×10^{-3}	0.90	E2
$3s^23p^2\ ^3P$	$3s3p^2\ (^3_2P)\ 3d\ ^5F$	0	2	7.465×10^{1}	1.06×10^{6}	4.41×10^{-6}	1.09×10^{-2}	0.99	E2
$3s^23p^2\ ^3P$	$3s3p^2\ (^3_2P)\ 3d\ ^5P$	0	2	7.130×10^{1}	1.10×10^{4}	4.19×10^{-8}	9.05×10^{-5}	1.00	E2
$3s^23p^2\ ^3P$	$3s3p^2\ (^3_2P)\ 3d\ ^3P$	0	2	7.076×10^{1}	8.79×10^{5}	3.30×10^{-6}	6.96×10^{-3}	0.98	E2
$3s^23p^2\ ^3P$	$3s3p^2\ (^3_2P)\ 3d\ ^3D$	0	2	6.808×10^{1}	4.52×10^{6}	1.57×10^{-5}	2.95×10^{-2}	0.98	E2
$3s^23p^2\ ^3P$	$3s3p^2\ (^1_2D)\ 3d\ ^3D$	0	2	6.552×10^{1}	3.05×10^{5}	9.81×10^{-7}	1.64×10^{-3}	1.10	E2
$3s^23p^2\ ^3P$	a	0	2	6.425×10^{1}	2.04×10^{5}	6.31×10^{-7}	9.97×10^{-4}	0.78	E2
$3s^23p^2\ ^3P$	$3s3p^2\ (^1_2D)\ 3d\ ^3P$	0	2	6.314×10^{1}	6.14×10^{4}	1.83×10^{-7}	2.75×10^{-4}	1.10	E2
$3s^23p^2\ ^3P$	$3s3p^2\ (^3_2P)\ 3d\ ^3F$	0	2	6.286×10^{1}	3.07×10^{3}	9.11×10^{-9}	1.35×10^{-5}	2.30	E2
$3s^23p^2\ ^3P$	$3s3p^2\ (^3_2P)\ 3d\ ^3D$	0	2	6.210×10^{1}	7.47×10^{5}	2.16×10^{-6}	3.08×10^{-3}	1.00	E2
$3s^23p^2\ ^3P$	$3s3p^2\ (^1_2D)\ 3d\ ^1D$	0	2	6.026×10^{1}	1.74×10^{5}	4.74×10^{-7}	6.17×10^{-4}	1.00	E2
$3s^23p^2\ ^3P$	$3s3p^2\ (^1S)\ 3d\ ^3D$	0	2	5.848×10^{1}	1.86×10^{3}	4.78×10^{-9}	5.69×10^{-6}	0.42	E2
$3s^23p^2\ ^3P$	$3s3p^2\ (^1S)\ 3d\ ^1D$	0	2	5.829×10^{1}	6.70×10^{4}	1.71×10^{-7}	2.01×10^{-4}	1.00	E2
$3s^23p^2\ ^3P$	$3s3p^2\ (^3_2P)\ 3d\ ^3P$	0	2	5.713×10^{1}	1.78×10^{5}	4.35×10^{-7}	4.83×10^{-4}	1.20	E2
$3s^23p^2\ ^3P$	$3s^23d^2\ ^3F$	0	2	5.532×10^{1}	3.26×10^{4}	7.48×10^{-8}	7.55×10^{-5}	0.89	E2
$3s^23p^2\ ^3P$	$3s3p^2\ (^3_2P)\ 3d\ ^1D$	0	2	5.373×10^{1}	1.51×10^{3}	3.27×10^{-9}	3.02×10^{-6}	2.60	E2
$3s^23p^2\ ^3P$	$3s^23d^2\ ^3P$	0	2	5.307×10^{1}	2.16×10^{1}	4.55×10^{-11}	4.05×10^{-8}	0.27	E2
$3s^23p^2\ ^3P$	$3s^23d^2\ ^1D$	0	2	5.267×10^{1}	2.47×10^{4}	5.13×10^{-8}	4.47×10^{-5}	0.83	E2

The letter "a" in the row k imply the unidentified level at position 65.

Table 4. Transition data for M1 and M2 transitions for Si-like Rb from $3s^23p^2\ ^3P_o$: levels and J for lower level i, upper level k, wavelength λ (in Å), transition rate A_{ji} (length form), oscillator strength f_{ij} (length form), line strength, S_{ij} (in unit a.u.) (length form).

Levels		J		MCDF2				Transition type
I	k	i	k	λ/Å	A_{ji}/s^{-1}	f_{ij}	S_{ij}	
$3s^23p^2\ ^3P$	$3s^23p^2\ ^3P$	0	1	1.266×10^{3}	7.51×10^{3}	5.41×10^{-6}	1.69×10^{0}	M1
$3s^23p^2\ ^3P$	$3s3p^2\ (^3_2P)\ 3d\ ^5F$	0	1	8.197×10^{1}	7.69×10^{1}	2.32×10^{-10}	4.71×10^{-6}	M1
$3s^23p^2\ ^3P$	$3s3p^2\ (^3_2P)\ 3d\ ^3P$	0	1	7.825×10^{1}	1.51×10^{2}	4.16×10^{-10}	8.04×10^{-6}	M1
$3s^23p^2\ ^3P$	$3s3p^2\ (^3_2P)\ 3d\ ^5D$	0	1	7.626×10^{1}	3.85×10^{1}	1.01×10^{-10}	1.90×10^{-6}	M1
$3s^23p^2\ ^3P$	$3s3p^2\ (^3_2P)\ 3d\ ^5P$	0	1	7.092×10^{1}	5.64×10^{2}	1.28×10^{-9}	2.24×10^{-5}	M1
$3s^23p^2\ ^3P$	$3p^4\ ^3P$	0	1	6.867×10^{1}	1.77×10^{2}	3.76×10^{-10}	6.39×10^{-6}	M1
$3s^23p^2\ ^3P$	$3s3p^2\ (^3_2P)\ 3d\ ^3D$	0	1	6.637×10^{1}	2.02×10^{2}	4.01×10^{-10}	6.58×10^{-6}	M1
$3s^23p^2\ ^3P$	$3s3p^2(^3_2P)\ 3d\ ^3D$	0	1	6.498×10^{1}	1.20×10^{-1}	2.28×10^{-13}	3.67×10^{-9}	M1
$3s^23p^2\ ^3P$	$3s3p^2\ (^1_2D)\ 3d\ ^3D$	0	1	6.476×10^{1}	4.21×10^{1}	7.95×10^{-11}	1.27×10^{-6}	M1
$3s^23p^2\ ^3P$	$3s3p^2\ (^1_2D)\ 3d\ ^3P$	0	1	6.386×10^{1}	3.44×10^{2}	6.32×10^{-10}	9.98×10^{-6}	M1
$3s^23p^2\ ^3P$	$3s3p^2\ (^1_2D)\ 3d\ ^3S$	0	1	6.238×10^{1}	1.94×10^{1}	3.39×10^{-11}	5.23×10^{-7}	M1
$3s^23p^2\ ^3P$	$3s3p^2\ (^1_2D)\ 3d\ ^1P$	0	1	6.119×10^{1}	4.29×10^{-1}	7.22×10^{-13}	1.09×10^{-8}	M1
$3s^23p^2\ ^3P$	$3s3p^2\ (^3_2P)\ 3d\ ^1P$	0	1	5.830×10^{1}	7.13×10^{0}	1.09×10^{-11}	1.57×10^{-7}	M1
$3s^23p^2\ ^3P$	$3s3p^2\ (^1S)\ 3d\ ^3D$	0	1	5.787×10^{1}	5.73×10^{-1}	8.63×10^{-13}	1.24×10^{-8}	M1
$3s^23p^2\ ^3P$	$3s3p^2\ (^3_2P)\ 3d\ ^3P$	0	1	5.586×10^{1}	1.33×10^{2}	1.86×10^{-10}	2.58×10^{-6}	M1
$3s^23p^2\ ^3P$	$3s^23d^2\ ^3P$	0	1	5.336×10^{1}	3.36×10^{2}	4.30×10^{-10}	5.68×10^{-6}	M1
$3s^23p^2\ ^3P$	$3s3p^{35}S^o$	0	2	2.009×10^{2}	2.67×10^{1}	8.07×10^{-10}	2.93×10^{0}	M2
$3s^23p^2\ ^3P$	$3s3p^{33}D^o$	0	2	1.607×10^{2}	5.12×10^{1}	9.91×10^{-10}	1.84×10^{0}	M2
$3s^23p^2\ ^3P$	$3s3p^{31}D^o$	0	2	1.378×10^{2}	1.56×10^{1}	2.23×10^{-10}	2.61×10^{-1}	M2
$3s^23p^2\ ^3P$	$3s3p^{33}P^o$	0	2	1.259×10^{2}	6.90×10^{-1}	8.20×10^{-12}	7.32×10^{-3}	M2
$3s^23p^2\ ^3P$	$3s^23p\ (^2_1P)\ 3d\ ^3F^o$	0	2	1.198×10^{2}	7.19×10^{1}	7.74×10^{-10}	5.95×10^{-1}	M2
$3s^23p^2\ ^3P$	$3s^23p\ (^2_1P)\ 3d\ ^3P^o$	0	2	1.079×10^{2}	1.53×10^{1}	1.33×10^{-10}	7.49×10^{-2}	M2
$3s^23p^2\ ^3P$	$3s^23p\ (^2_1P)\ 3d\ ^1D^o$	0	2	9.974×10^{1}	1.45×10^{1}	1.08×10^{-10}	4.81×10^{-2}	M2
$3s^23p^2\ ^3P$	$3s^23p\ (^2_1P)\ 3d\ ^3D^o$	0	2	9.649×10^{1}	1.05×10^{1}	7.36×10^{-11}	2.96×10^{-2}	M2

We adopt the length gauge in our calculations, as length results are expected to be more accurate than the velocity results. The velocity results are much more sensitive to the choice of configurations while the length form for transitions is stabler. The value of the ratio of vel./len. form indicates the calculation precision as it indicates the accuracy of f- or A-values. As seen from Table 3, the vel./len ratio in our case is generally within 10% of unity for most of the strong transitions ($f \geq 0.1$) listed in Table 3. For some strong transitions such as $3s^23p^2\ ^3P_0$–$3s3p^3\ ^3D^o_1$, $3s^23p^2\ ^3P_0$–$3s3p^3\ ^3S^o_1$, $3s^23p^2\ ^3P_0$–$3s^23p\ (^2_1P)\ 3d\ ^3D^o_1$, etc., the ratio is exactly unity. For weaker transitions ($f \sim 10^{-5}$ or less), such as $3s^23p^2\ ^3P_0$–$3s^23p^2\ ^3P_2$, $3s^23p^2\ ^3P_0$–$3s^23p^2\ ^1D_2$, $3s^23p^2\ ^3P_0$–$3s3p^23d\ ^5F_2$, and $3s^23p^2\ ^3P_0$–$3s^23d^2\ ^3P_2$, the ratio is higher. As the discrepancy between both length and velocity forms sometimes may be large for weaker transitions, it does not affect the overall accuracy of our calculations because weaker transitions are found to be sensitive to the cancellation effects among mixing coefficients and are not very important. Most of the spectral lines are found to be obtained in EUV (100–1200 Å) and x-ray (< 100 Å) regions. Further we notice a sudden decrease in wavelength for transition from 474.2 Å to 83.32 Å in Table 3 when the upper level changes from $3s^23p^2\ ^1D_2$ to $3p^4\ ^3P_2$ and in Table 4 for levels from upper level $3s^23p^2\ ^3P_1$ to $3s3p^2\ (^3_2P)\ 3d\ ^5F_1$ from 1266 Å to 81.97 Å which may be due to the increase in the force of repulsion between core and valence electrons through exciting an electron from 3p to 3d orbital, thereby increasing the transition energy.

Table 5. Comparison of computed wavelengths (in Å) with observed wavelengths from NIST and other theories for transitions from $3s^23p^2\ ^3P_{0,1,2}$ to selected upper levels.

S. No.	Levels		J		λ/Å	λ/Å	λ/Å	Transition type
	Lower	Upper	i	k	This work	NIST	Ref. [20]	
1	$3s^23p^2\ ^3P$	$3s^23p^2\ ^3P$	0	1	1.266×10^3	1.249×10^3	1.259×10^3	M1
2	$3s^23p^2\ ^3P$	$3s^23p^2\ ^1D$	2	2	9.683×10^2	9.686×10^2		M1
3	$3s^23p^2\ ^3P$	$3s^23p^2\ ^1D$	1	2	7.583×10^2	7.640×10^2		M1
4	$3s^23p^2\ ^3P$	$3s^23p^2\ ^1S$	1	0	4.852×10^2	4.944×10^2		M1
5	$3s^23p^2\ ^3P$	$3s^23p^2\ ^3P$	1	2	3.497×10^3	3.619×10^3		M1
6	$3s^23p^2\ ^3P$	$3s3p^3\ ^3D^o$	0	1	1.637×10^2		1.631×10^2	E1
7	$3s^23p^2\ ^3P$	$3s3p^3\ ^3P^o$	0	1	1.370×10^2		1.366×10^2	E1
8	$3s^23p^2\ ^3P$	$3s3p^3\ ^1P^o$	0	1	1.047×10^2		1.184×10^2	E1
9	$3s^23p^2\ ^3P$	$3s3p^3\ ^3S^o$	0	1	1.186×10^2		1.069×10^2	E1
10	$3s^23p^2\ ^3P$	$3s^23p\ (^2_1P)\ 3d\ ^3P^o$	0	1	9.787×10^1		1.045×10^2	E1
11	$3s^23p^2\ ^3P$	$3s^23p\ (^2_1P)\ 3d\ ^3D^o$	0	1	1.072×10^2		9.761×10^1	E1
12	$3s^23p^2\ ^3P$	$3s^23p\ (^2_1P)\ 3d\ ^1P^o$	0	1	8.827×10^1		8.822×10^1	E1
13	$3s^23p^2\ ^3P$	$3s3p^{33}S^o$	2	1	1.360×10^2	1.378×10^2		E1
14	$3s^23p^2\ ^3P$	$3s^23p\ (^2_1P)\ 3d\ ^3P^o$	2	2	1.221×10^2	1.232×10^2		E1
15	$3s^23p^2\ ^1D$	$3s^23p\ (^2_1P)\ 3d\ ^3D^o$	2	2	1.211×10^2	1.223×10^2		E1
16	$3s^23p^2\ ^3P$	$3s^23p\ (^2_1P)\ 3d\ ^3P^o$	1	2	1.180×10^2	1.192×10^2		E1
17	$3s^23p^2\ ^1D$	$3s^23p\ (^2_1P)\ 3d\ ^1F^o$	2	3	1.128×10^2	1.143×10^2		E1
18	$3s^23p^2\ ^3P$	$3s^23p\ (^2_1P)\ 3d\ ^3D^o$	2	3	1.103×10^2	1.113×10^2		E1
19	$3s^23p^2\ ^3P$	$3s^23p\ (^2_1P)\ 3d\ ^1D^o$	1	2	1.083×10^2	1.094×10^2		E1
20	$3s^23p^2\ ^3P$	$3s^23p\ (^2_1P)\ 3d\ ^1F^o$	2	3	1.010×10^2	1.022×10^2		E1
21	$3s^23p^2\ ^3P$	$3s^23p^2\ ^3P$	0	2	9.29×10^2		9.228×10^2	E2
22	$3s^23p^2\ ^3P$	$3s^23p^2\ ^1D$	0	2	4.74×10^2		4.726×10^2	E2

In Table 5, we compare our calculated wavelengths of Rb XXIV with those published by Huang[20] and those compiled by NIST. We observe that our results are in reasonable agreement with those present in the literature. The maximum disagreement between our calculated MCDF transition wavelengths and the NIST results is 3.37% while 11.5% with those of Huang.[20] Also, the mean ratio $\lambda_{\text{Thiswork}}/\lambda_{\text{exp.}}$ is found to be 0.9897, which indicates the accuracy of our results. The difference between our results and Huang's[20] are mainly because of the different amounts of CI included. Our results are expected to be more reliable as we have included larger CI for our calculations. We plot our wavelengths and NIST values in Fig. 1. The horizontal axis represents 'Line Label' corresponding to transition labels as indicated in the first column of Table 5.

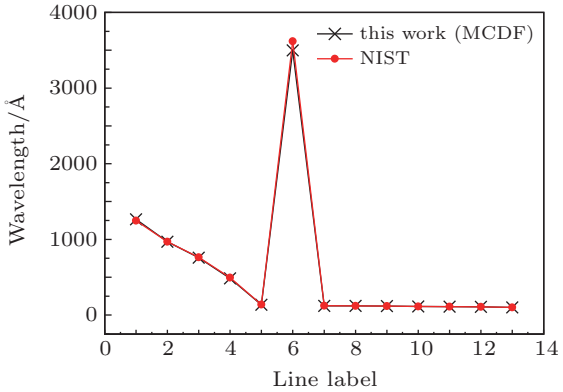


Fig. 1. (color online) MCDF (cross) and observed NIST (circle) wavelengths versus transition.

From Table 6, we find that our *A*-values are in reasonable agreement with NIST values except for transitions $3s^23p^2\ ^3P_2$–$3s3p\ ^3S^o_1$ and $3s^23p^2\ ^3P_1$–$3s^23p3d\ ^1D^o_2$. A reassessment of transition probability data for these transitions for Rb XXIV on the NIST website is desirable. Our results are comparable to those of Huang for some transitions while for some other transitions there is a huge discrepancy. Our *A*-values from the MCDF and FAC agree well with each other, showing that the CI included in the calculations is sufficient enough to produce accurate radiative rates. Table 7 shows a comparison of our *f*-values from ground level $3s^23p^2\ ^3P_o$ with the results presented by Huang[20] using MCDF and by Charro *et al.*[27] using RQDO. Similarly, Table 8 shows a comparison of line strength results with the results given by Huang,[20] the only available results in the literature.

Table 6. Comparison of computed transition probabilities A_{ji}/s^{-1} with those from NIST and other theories for transition from $3s^23p^2\ ^3P_{0,1,2}$ to selected upper levels.

Levels		*J*		A_{ji}/s^{-1} This work		NIST	A_{ji}/s^{-1}	Transition type
Lower	Upper	*i*	*k*	MCDF	FAC		Ref. [20]	
$3s^23p^2\ ^3P$	$3s^23p^2\ ^3P$	0	1	7.51×10^3		7.8×10^3	7.57×10^3	M1
$3s^23p^2\ ^3P$	$3s3p^3\ ^3D^o$	0	1	8.34×10^9	8.43×10^9		8.57×10^9	E1
$3s^23p^2\ ^3P$	$3s3p^3\ ^3P^o$	0	1	4.02×10^9	4.05×10^9		4.02×10^9	E1
$3s^23p^2\ ^3P$	$3s3p^3\ ^1P^o$	0	1	9.32×10^9	1.06×10^{10}		2.17×10^{10}	E1
$3s^23p^2\ ^3P$	$3s3p^3\ ^3S^o$	0	1	2.29×10^{10}	2.24×10^{10}		1.16×10^{11}	E1
$3s^23p^2\ ^3P$	$3s^23p\ (^2_1P)\ 3d\ ^3P^o$	0	1	3.12×10^8	2.79×10^8		1.24×10^{10}	E1
$3s^23p^2\ ^3P$	$3s^23p\ (^2_1P)\ 3d\ ^3D^o$	0	1	1.18×10^{11}	1.15×10^{11}		2.82×10^8	E1
$3s^23p^2\ ^3P$	$3s^23p\ (^2_1P)\ 3d\ ^1P^o$	0	1	1.67×10^9	1.55×10^9		1.63×10^9	E1
$3s^23p^2\ ^3P$	$3s^23p^2\ ^3P$	0	2	7.80×10^0	7.87×10^0		8.27×10^0	E2
$3s^23p^2\ ^3P$	$3s^23p^2\ ^1D$	0	2	2.42×10^{-5}			8.41×10^{-2}	E2
$3s^23p^2\ ^3P$	$3s^23p^2\ ^1D$	2	2	1.08×10^4	1.08×10^4	1.1×10^4		M1
$3s^23p^2\ ^3P$	$3s^23p^2\ ^1D$	1	2	1.28×10^4	1.28×10^4	1.3×10^4		M1
$3s^23p^2\ ^3P$	$3s^23p^2\ ^1S$	1	0	7.06×10^4	7.02×10^4	6.9×10^4		M1
$3s^23p^2\ ^3P$	$3s^23p^2\ ^3P$	1	2	1.84×10^2	1.81×10^2	1.6×10^2		M1
$3s^23p^2\ ^3P$	$3s3p^{33}S^o$	2	1	8.29×10^{10}	8.23×10^{10}	4.8×10^9		E1
$3s^23p^2\ ^3P$	$3s^23p\ (^2_1P)\ 3d\ ^3P^o$	2	2	3.90×10^{10}	3.86×10^{10}	3.9×10^{10}		E1
$3s^23p^2\ ^1D$	$3s^23p\ (^2_1P)\ 3d\ ^3D^o$	2	2	1.02×10^{11}	1.00×10^{11}	1.7×10^{10}		E1
$3s^23p^2\ ^3P$	$3s^23p\ (^2_1P)\ 3d\ ^3P^o$	1	2	6.27×10^{10}	6.20×10^{10}	6.2×10^{10}		E1
$3s^23p^2\ ^1D$	$3s^23p\ (^2_1P)\ 3d\ ^1F^o$	2	3	1.12×10^{11}	1.11×10^{11}	1.1×10^{11}		E1
$3s^23p^2\ ^3P$	$3s^23p\ (^2_1P)\ 3d\ ^3D^o$	2	3	1.20×10^{11}	1.19×10^{11}	1.2×10^{11}		E1
$3s^23p^2\ ^3P$	$3s^23p\ (^2_1P)\ 3d\ ^1D^o$	1	2	5.91×10^{10}	5.87×10^{10}	2.5×10^8		E1
$3s^23p^2\ ^3P$	$3s^23p\ (^2_1P)\ 3d\ ^1F^o$	2	3	2.41×10^{10}	2.37×10^{10}	2.3×10^{10}		E1

Table 7. Comparison of computed oscillator strengths f_{ij} with those from NIST and different theories for transition from $3s^23p^2\ ^3P_0$ to selected upper levels.

Levels		*J*		f_{ij}	f_{ij}	Transition type
Lower	Upper	*i*	*k*	This work	Ref. [20]	
$3s^23p^2\ ^3P$	$3s^23p^2\ ^3P$	0	1	5.41×10^{-6}	5.403×10^{-6}	M1
$3s^23p^2\ ^3P$	$3s3p^3\ ^3D^o$	0	1	1.01×10^{-1}	1.026×10^{-1}	E1
$3s^23p^2\ ^3P$	$3s3p^3\ ^3P^o$	0	1	3.39×10^{-2}	3.38×10^{-2}	E1
$3s^23p^2\ ^3P$	$3s3p^3\ ^1P^o$	0	1	4.60×10^{-2}	1.37×10^{-1}	E1
$3s^23p^2\ ^3P$	$3s3p^3\ ^3S^o$	0	1	1.45×10^{-1}	5.95×10^{-1}	E1
$3s^23p^2\ ^3P$	$3s^23p\ (^2_1P)\ 3d\ ^3P^o$	0	1	1.34×10^{-3}	6.08×10^{-2}	E1
$3s^23p^2\ ^3P$	$3s^23p\ (^2_1P)\ 3d\ ^3D^o$	0	1	6.08×10^{-1}	1.21×10^{-3}	E1
$3s^23p^2\ ^3P$	$3s^23p\ (^2_1P)\ 3d\ ^1P^o$	0	1	5.86×10^{-3}	5.70×10^{-3}	E1
$3s^23p^2\ ^3P$	$3s^23p^2\ ^3P$	0	2	5.05×10^{-9}	5.28×10^{-9}	E2
$3s^23p^2\ ^3P$	$3s^23p^2\ ^1D$	0	2	4.09E-15	1.41×10^{-11}	E2
$3s^23p^2\ ^1D$	$3s^23p\ (^2_1P)\ 3d\ ^1D^o$	2	2	4.11×10^{-2}	[a]1.51×10^{-1}	E1
				0	[b]1.75×10^{-2}	
$3s^23p^2\ ^1D$	$3s^23p\ (^2_1P)\ 3d\ ^1F^o$	2	3	2.25×10^{-1}	[a]3.50×10^{-1}	E1
				0	[b]3.00×10^{-1}	

[a]Charro using RQDO,[27] [b]Huang using MCDF.[20]

Table 8. Comparison of computed line strengths S_{ij} (in unit a.u.) with those from NIST and different theories for transition from $3s^23p^2\ ^3P_0$ to selected upper levels.

Levels		J		S_{ij} (MCDF)	S_{ij}	Transition type
Lower	Upper	i	k	This work	Ref. [20]	
$3s^23p^2\ ^3P$	$3s^23p^2\ ^3P$	0	1	1.69×10^{0}	1.68×10^{0}	M1
$3s^23p^2\ ^3P$	$3s3p^3\ ^3D^o$	0	1	5.42×10^{-2}	5.51×10^{-2}	E1
$3s^23p^2\ ^3P$	$3s3p^3\ ^3P^o$	0	1	1.53×10^{-2}	1.52×10^{-2}	E1
$3s^23p^2\ ^3P$	$3s3p^3\ ^1P^o$	0	1	1.59×10^{-2}	5.35×10^{-2}	E1
$3s^23p^2\ ^3P$	$3s3p^3\ ^3S^o$	0	1	5.66×10^{-2}	2.09×10^{-1}	E1
$3s^23p^2\ ^3P$	$3s^23p\ (^2_1P)\ 3d\ ^3P^o$	0	1	4.33×10^{-4}	2.09×10^{-2}	E1
$3s^23p^2\ ^3P$	$3s^23p\ (^2_1P)\ 3d\ ^3D^o$	0	1	2.15×10^{-1}	3.88×10^{-4}	E1
$3s^23p^2\ ^3P$	$3s^23p\ (^2_1P)\ 3d\ ^1P^o$	0	1	1.70×10^{-3}	1.66×10^{-3}	E1
$3s^23p^2\ ^3P$	$3s^23p^2\ ^3P$	0	2	2.41×10^{-2}	2.47×10^{-2}	E2
$3s^23p^2\ ^3P$	$3s^23p^2\ ^1D$	0	2	2.60×10^{-9}	8.85×10^{-6}	E2

5. Lifetimes

Table 1 includes the values of radiative lifetimes for all 97 levels in the length gauge from our calculations, and these values are obtained from our radiative transition probabilities A_{ji} which are obtained from the following expression:

$$\tau_j = \frac{1}{\sum_i A_{ji}}, \tag{13}$$

where the summation over i refers to the sum of all accessible final states and the values of $\Delta E = E_j - E_i$. Lifetime calculations include A-values from all types of transitions, i.e., E1, E2, M1, and M2. Lifetimes for the levels $3s3p^3\ ^3P_1$, $3s3p^3\ ^3P_2$, $3s3p^3\ ^1D_2$, $3s3p^3\ ^1S_0$, $3s3p^3\ ^5S_0$, and $3s^23p\ (^2_1P)\ 3d\ ^3F_0$ are larger than those for other levels. As equation (13) provides a means of comparing theory (transition probability) with experiment (lifetimes), our results will be useful for experimentalists in future to make comparison between experimental results and theoretical values and also to check the accuracy of calculations.

6. Conclusions

In this work, fine structure energy levels, oscillator strengths, line strengths and transition probabilities for transitions between the levels belonging to $3s^23p^2$, $3s^23p3d$, $3s3p^3$, $3p^4$, $3s3p^23d$, and $3s^23d^2$ of Rb XXIV are obtained by using MCDF wavefunctions. We perform two independent calculations by using MCDF and FAC to compare energy levels and transition probabilities. Comparisons are performed between these two sets of energy levels, as well as with other available results, showing that they are in good agreement with each other. Though all the care is taken to identify the levels according to the strengths of eigenvectors, still there always lies a possibility of their redesignation. We also conduct a comparison for other parameters, especially for transition wavelengths. In general, the accuracies of listed wavelength values are assessed to be within 3.37%. Further, the lifetimes of all 97 levels are also reported.

We believe that our atomic data have been the most extensive and definitive to date and will be useful in controlled thermonuclear fusion research, astrophysical applications and in technical plasma modeling.

References

[1] Chandra x-ray Observatory. Available at http://chandra.harvard.edu/
[2] The Solar and Heliospheric Observatory. Available at http:// sohowww.nascom.nasa.gov/
[3] Behringer K 2000 in *Atomic and Molecular Data and their Applications*, eds. Berrington K A and Bell K L (New York: AIP) p. 142
[4] Liedahl D A, Beiersdorfer P, Brown G V, Utter S B, Khan S M, Gu M F and Savin D W 1998 *Laboratory Space Science Workshop*, April 1–3, 1998, Washington, NASA, USA, p. 85
[5] Edlén B 1983 *Phys. Scr. T* **8** 5
[6] Träbert E, Heckmann P H, Hutton R and Martinson I 1988 *J. Opt. Soc. Am. B* **5** 2173
[7] Ellis D G, Martinson I and Träbert E 1900 *Comm. At. Mol. Phys.* **22** 241
[8] Seaton M J 1987 *J. Phys. B: At. Mol. Opt. Phys.* **20** 6363
[9] Widing K G, Sandlin G D and Cowan R D 1971 *Astrophys. J.* **169** 405
[10] Malinovsky M and Heroux L 1973 *Astrophys. J.* **181** 1009
[11] Behring W E, Cohen L, Doschek G A and Feldman U 1976 *Astrophys. J.* **203** 521
[12] Fawcett B C 1971 *J. Phys. B: At. Mol. Opt. Phys.* **4** 1577
[13] McWhirter R W R and Summers H P 1984 *Appl. At. Coll. Ph.* **2** 51
[14] Brage T, Judge P G and Brekke P 1996 *Astrophys. J.* **464** 1030
[15] Biémont E 1986 *J. Opt. Soc. Am. B* **3** 163
[16] Biémont E 1986 *Phys. Scr.* **33** 324
[17] Bromage G E 1980 *Astron. Astrophys.* **41** 79
[18] Bromage G E, Cowan R D and Fawcett B C 1978 *Mon. Not. R. Astron. Soc.* **183** 19
[19] Cowan R D 1981 in *The Theory of Atomic Structure and Spectra* (Berkeley, CA: University of California Press)
[20] Huang K N 1985 *At. Data Nucl. Data Tables* **32** 503
[21] Fawcett B C 1987 *At. Data Nucl. Data Tables* **36** 129
[22] Hibbert A 1988 *Phys. Scr.* **38** 87
[23] Nahar S N 1993 *Phys. Scr.* **48** 297
[24] Kohstall C, Fritzsche S, Fricke B and Sepp W D 1998 *At. Data Nucl. Data Tables* **70** 63
[25] Nahar S N 1993 *Phys. Scr.* **48** 297
[26] Nahar S N 1999 *At. Data Nucl. Data Tables* **72** 129
[27] Charro E, Martin I and Lavin C 1997 *Astron. Astrophys. Suppl. Ser.* **124** 397
[28] Saha B, Das A K and Mukherjee P K 2001 *Eur. Phys. J. D* **14** 33
[29] Saha B, Mukherjee T K, Das A K and Mukherjee P K 2003 *Int. J. Quantum Chem.* **91** 626
[30] Landi E and Bhatia A K 2003 *Astrophys. J.* **589** 1075
[31] Tayal V and Gupta G P 2007 *Phys. Scr.* **75** 331
[32] Froese Fisher C, Tachiev G and Irimia A 2006 *At. Data Nucl. Data Tables* **92** 607

[33] Ishikawa Y and Vilkas M J 2001 *Phys. Rev. A* **63** 042506
[34] Ishikawa Y and Vilkas M J 2003 *Phys. Rev. A* **68** 012503
[35] Tayal V and Gupta G P 2007 *Phys. Scr.* **75** 331
[36] Gupta G P and Msezane A Z 2011 *Phys. Scr.* **83** 055301
[37] Gupta G P and Msezane A Z 2012 *Phys. Scr.* **86** 015303
[38] Träbert E, Pinnington E H, Kernahan J A, Doerfert J, Granzow J, Heckmann P H and Hutton H J 1996 *J. Phys. B: At. Mol. Opt. Phys.* **29** 2647
[39] Fawcett B C and Hayes R W 1972 *J. Phys. B: At. Mol. Opt. Phys.* **5** 366
[40] Kastner S O, Swartz M, Bhatia A K and Lapides J 1978 *J. Opt. Soc. Am.* **68** 1558
[41] Träbert E, Grieser M, Krantz C, Repnow R, Wolf A, Diaz F J, Ishikawa Y and Santana J A 2012 *J. Phys. B: At. Mol. Opt. Phys.* **45** 215003
[42] Khan M A 1978 *Opt. Commun.* **27** 242
[43] Sugar J, Kaufmann V and Rowan W L 1990 *J. Opt. Soc. Am. B* **7** 152
[44] Wyart J F TFR Group 1988 *Phys. Scr.* **37** 66
[45] Jupén C, Martinson I and Denne-Hinnov B 1991 *Phys. Scr.* **44** 562
[46] Träbert E 1993 *Phys. Scr.* **48** 699
[47] Träbert E 1986 *Z. Phys. D* **2** 213
[48] Träbert E 1987 *Z. Phys. D* **5** 125
[49] Rodrigues G C, Indelicato P, Santos J P, Patté P and Parente F 2004 *At. Data Nucl. Data Tables* **86** 117
[50] Carlson Thomas A, Nestor C W, Neil Wasserman J R and McDowell J D 1970 *Atomic Data* **2** 63
[51] Sugar J and Kaufmann V 1984 *J. Opt. Soc. Am. B* **1** 218
[52] Biémont E, Frémat Y and Quinet P 1999 *At. Data Nucl. Data Tables* **71** 117
[53] Aguiar Julio C and Di Rocco Héctor O 2014 *J. Quantum Spectrosc. Radiat. Transfer* **49** 1
[54] Kramida A, Ralchenko Yu, Reader J, NIST ASD Team, 2014 *NIST Atomic Spectra Database*, Version 5.2, Online available at: http://physics.nist.gov/asd
[55] Grant I P, Mckenzie B J, Norrington P H, Mayers D F and Pyper N C 1980 *Comput. Phys. Commun.* **21** 207
[56] Norrington P H 2009 http://www.am.qub.ac.uk/DARC/
[57] Quinet P 2012 *J. Phys. B: At. Mol. Opt. Phys.* **45** 025003
[58] Gu M F 2008 *Can. J. Phys.* **86** 675
[59] Singh A K, Aggarwal S and Mohan M 2013 *Phys. Scr.* **88** 035301
[60] Aggarwal S, Singh J and Mohan M 2013 *At. Data Nucl. Data Tables* **99** 704
[61] Aggarwal K M, Keenan F P and Msezane A Z 2003 *At. Data Nucl. Data Tables* **85** 453
[62] Goyal A, Khatri I, Aggarwal S, Singh A K and Mohan M 2013 *Can. J. Phys.* **91** 394
[63] Aggarwal S, Jha A K S, Khatri I, Singh N and Mohan M 2015 *Chin. Phys. B* **24** 053201
[64] Grant I P 1988 in *Relativistic Effects in Atoms and Molecules*, ed. Wilson S (*Methods in Computational Chemistry*), Vol. 2 (New York: Plenum Press), pp. 1–71
[65] Gu M F 2003 *Astrophys. J.* **582** 1241
[66] Flambaum V V and Sushkow O P 1978 *J. Quantum. Spectros. Radiat. Transfer* **20** 569
[67] Biémont E and Hansen J E 1986 *Phys. Scr.* **33** 117
[68] Dembczynski J and Rebel H 1984 *Physica* **125C** 341